UDC 662.2.546.47'21':539.26

SHOCK-WAVE SYNTHESIS OF HIGH-DENSITY MODIFICATIONS OF ZINC OXIDE (REVIEW)

A. N. Tsvigunov,[1] A. S. Krasikov,[1] and V. G. Khotin[1]

Translated from *Steklo i Keramika*, No. 1, pp. 22 – 29, January, 2010.

The results of x-ray diffraction studies of preserved zincite samples subjected to dynamic compression (28 GPa) and the powder patterns of hydrothermally grown ZnO crystals are presented.
Three new modifications have been synthesized: ZnO(I, II, III). The x-ray diffraction pattern of ZnO(I) is indexed in the hexagonal unit cell with $a = 4.121(2)$ Å, $c = 15.114(5)$ Å, $V = 222.3$ Å^3, $Z = 12$, $\rho_{calc} = 7.293$ g/cm^3, Fedorov group $P6_3/mmc$. The x-ray diffraction data for ZnO(II) are indexed in an orthorhombic subcell with $a = 5.997(2)$ Å, $b = 5.267(1)$ Å, $c = 2.369(1)$ Å, $V = 74.8$ Å^3, $Z = 4$, $\rho_{calc} = 7.222$ g/cm^3. The x-ray diffraction pattern of ZnO(III) is indexed in the primitive monoclinic cell with $a = 7.931(8)$ Å, $b = 7.911(4)$ Å, $c = 2.995(1)$ Å, $\beta = 91.07(4)°$, $V = 188$ Å^3, $Z = 8$, $\rho_{calc} = 5.749$ g/cm^3.

Key words: zinc oxide, shock compression, unit-cell parameters.

According to the geometric model an ionic crystal consists of ionic spheres with a definite radius. Each coordination polyhedron (icosahedron, cube, octahedron, tetrahedron, regular triangle) has a critical (minimum) ratio R_c/R_a of the radii of the cation and anion with which it can be formed (anions touch cations as well as one another).

The probability of any particular coordination of the cations can be estimated by means of the Magnus – Goldschmidt criterion: a coordination polyhedron forms in a structure if the ratio R_c/R_a is greater than a critical value.

The ratio $R_c/R_a = 1$ for an icosahedron, 0.731 for a cube, 0.414 for an octahedron, 0.225 for a tetrahedron, and 0.155 for a triangle.

The environment of zinc can be octahedral in compounds containing oxygen, since the ratio of the ionic radii of zinc (0.74 Å) and oxygen (1.36 Å) is 0.544 and falls into the interval 0.414 – 0.732.

A solid solution with NaCl type structure is formed when zincite dissolves in CoO and NiO. Synthesis of pyroxene $ZnSiO_3$ according to the reaction

$$ZnO + SiO_2 \rightarrow ZnSiO_3$$

is accompanied by an increase of the coordination number $ZnO_4 \rightarrow ZnO_6$. However, at atmospheric pressure the environment of zinc in most compounds is tetrahedral. The enthalpy of a coordination change $(ZnO_4 \rightarrow ZnO_6)\Delta H = 24.5 \pm 3.6$ kJ/mole, calculated from thermochemical data for a series of compounds and solid solutions, indicates that the preferred symmetry of oxygen atoms surrounding zinc is tetrahedral [1].

A tetrahedral environment around zinc is observed in zinc sulfide under normal conditions. Sphalerite and wurtzite modifications of this compound, where each atom is surrounded by an almost regular tetrahedron formed by atoms of the other type, are encountered in nature. Sphalerite (α-ZnS) crystallizes in the cubic system with $a = 5.409$ Å, $V = 158.2$ Å^3, $Z = 4$, volume per formula unit $(V/Z) = 39.6$ Å^3, and Fedorov group $F\bar{4}3m$ (3C).

The lattice of α-ZnS can be regarded as two face-centered cubic lattices shifted relative to one another by one-fourth the diagonal of a cube. The zinc and sulfur atoms in the sphalerite structure occupy the sites of these sublattices, which possess the symmetry of a tetrahedron ($\bar{4}3m$).

In the space group $F\bar{4}3m$ the number of formula units, equal to 4 (symmetry value), creates a combination of positions 4(a) + 4(c) with $\bar{4}3m$ symmetry [2]. Zinc atoms occupy the position 4(a) : (000) and sulfur atoms occupy 4(c) : (1/4 1/4 1/4). The ZnS_4 and SZn_4 tetrahedra are in layers parallel to one another in a ratio with the requirements of cubic tight packing (Fig. 1).

Tight-packed layers of zinc atoms alternate with tight-packed layers of sulfur atoms. Each layer occupies half the tetrahedral voids between the top- and bottom-lying layers.

The combinations of the positions 4(a) + 4(b) = 4(c) + 4(d) with zinc atoms in the positions 4(a) and 4(c) lead to the Fedorov group $Fm\bar{3}m$ (NaCl type structurre).

[1] D. I. Mendeleev Russian Chemical Technology University, Moscow, Russia.

If the atoms occupying the indicated positions are identical, then the symmetry increases to $Fd\bar{3}m$. Diamond, silicon, pyrochlore, Laves phases of $MgCu_2$, and noble spinel $MgAl_2O_4$ all crystallize in the group $Fd\bar{3}m$. The space group $F4\bar{3}m$ is a common subgroup of $Fm\bar{3}m$ and $Fd\bar{3}m$: $Fm\bar{3}m \supset Fd\bar{3}m \supset F\bar{4}3m$.

In a previous work [3] the present authors were able to synthesize simultaneously two compounds — high-temperature and pressure mineral $MgAl_2O_4$ and high-density cubic Laves phase $MgCu_2$ — with the Fedorov group $Fd\bar{3}m$ by shock-wave compression of three substances (Al, MgO, Cu) with the space symmetry group $Fm\bar{3}m$ according to the reaction

$$2Al + 4MgO + 6Cu \rightarrow MgAl_2O_4 + 3MgCu_2.$$

In 1912 E. Allen and J. Crenshaw established that sphalerite (3C) is stable at temperatures below 1020°C, while wurtzite β-ZnS is known at higher temperatures. The transformation at 1020°C is reversible. This temperature is still the generally accepted temperature of the sphalerite-wurtzite transformation. The tetrahedra in the wurtzite structure have hexagonal packing (see Fig. 1). The parameters of the hexagonal unit cell are $a = 3.811$ Å, $c = 6.234$ Å, $c/a = 1.636$, $V = 78.4$ Å^3, $Z = 2$; the molecular volume (V/Z) equals 39.3 Å^3; the Fedorov group is $P6_3mc$ (2H). The phase transformation $3C \rightarrow 2H$ is accompanied by a decrease of the Gibbs energy.

The results of high-temperature single-crystal x-ray diffraction measurements and differential thermal analysis showed that the polymorphous transformation wurtzite → sphalerite and the reverse transformation occur via the intermediate polytypic modification 4H [4].

The chalcogenide minerals CdS, CdSe, ZnSe, ZnTe, and MnS can crystallize in sphalerite and wurtzite type structures. The polymorphous modifications with a hexagonal wurtzite lattice usually form at high temperature and the modifications with cubic structure form at lower temperatures. The molecular volumes of these modifications are approximately the same.

The lattice energies of the wurtzite and sphalerite structures were calculated in [5] for compounds of the type AB whose ions are isoelectronic to inert gas atoms. The calculations were performed on the basis of the Born – Mayer theory for ionic solids taking account of the three-point interaction to first and second orders of perturbation theory. For compounds with a stable sphalerite structure the energy of the crystal lattice is several percent lower than that of the wurtzite type lattice. The difference of the lattice energies of these structures in compounds with stable wurtzite structure is about 1%.

In the mineral greenockite CdS the stable phase possesses wurtzite type structure and the metastable phase possesses sphalerite type structure. The CdS phase with sphalerite structure forms from the stable phase under shear stresses (grinding in a mortar). The color changes from yellow (wurtzite) to red (sphalerite).

At atmospheric pressure ZnO (zincite) crystallized in a wurtzite structure with hexagonal packing of the oxygen ions.

The zinc and oxygen ions in wurtzite form ZnO_4, OZn_4 coordination polyhedral – tetrahedra. The parameters of the hexagonal unit cell are $a = 3.2539(1)$ Å, $c = 5.2098(3)$ Å, $c/a = 1.6011$, $V = 47.77$ Å^3; the Fedorov symmetry group is $P6_3mc$; the experimental density is 5.642(12) g/cm^3; the number of formula units (Z) is 2; and, the molecular volume 23.89 Å^3.

The zinc and oxygen atoms occupy equivalent monovariant two-fold positions (3m) – 2b:

$$\text{Zn} — 1/3, 2/3, 0; 2/3, 1/3, 1/2;$$
$$\text{O} — 1/3, 2/3, Z; 2/3, 1/3, 1/2 + Z.$$

For the wurtzite structure with a regular tetrahedron $c/a = 1.633$ and $Z = 0.375$. If the condition $4a^2 = (12u - 3)c^2$, where u is the coordinate of the Z atom of oxygen relative to the zinc atom at the position (0 0 0), is not satisfied in this structure, then there is a small difference between one metal – oxygen distance and the other three [6]. In zincite the coordinate $Z = 0.3826$; the three distances equal 1.937 Å and the fourth one is 1.992 Å [7].

In 1932 W. Bragg proposed that zinc oxide can crystallize in the sphalerite structure (ICPDS 65-2880). For equal molecular volumes of the polymorphous modifications of ZnO (3C and 2H) the unit cell parameter of ZnO (3C) is determined by the expression $a_c = (\sqrt{3}\, a_h^2\, c_h)^{1/3}$, where $a_h = 3.254$ Å, $c_h = 5.210$ Å, and $a_c = 4.572$ Å.

Subsequently, an electron-microscopic study of ultrathin layers of natural ZnO crystals revealed its modification with the cubic lattice of sphalerite. Analysis of the micro-diffraction patterns (sections of the reciprocal lattice with axes [011]*, [200]*, [020]*, [211]*, and others) made it possible to determine the true unit-cell parameter: $a = 5.587$ Å [8].

Zincite is an interstitial phase $Zn_{1+\delta}O$ and possesses the properties of an n-type semiconductor with average resistivity $(6 - 9) \times 10^4\ \Omega \cdot$ cm and conduction activation energy 3.2 ± 2 eV at room temperature. In addition, it manifests the properties of a catalyst and luminophore [9, 10].

Zincite is the strongest piezoelectric of all semiconducting materials. These properties depend strongly on the conditions of the preliminary heat treatment of ZnO.

Uncalcinated ZnO luminesces very weakly. Calcination in vacuum at temperatures above 700°C increased the total intensity of the luminescence considerably. As the heating temperature decreases to 600°C and below the luminescence properties of ZnO samples remain practically the same as for uncalcinated samples. Calcination of ZnO in zinc, magnesium, and lead vapors sharply intensifies the luminescence. A. V. Frost was the first to discover the difference in the cata-

lytic activity of ZnO samples preheated at different temperatures.

Calcination of zincite in zinc vapor at 800°C and zinc pressure from 6×10^{-5} to 2×10^{-2} mm Hg for 3 h increases the zinc content in the initial ZnO by a factor 11. Heat treatment of ZnO in vacuum also increases the zinc content but to a lesser extent — by a factor of 3.6. Under these conditions ZnO undergoes thermal dissociation — its lattice becomes a source of zinc atoms [9]. The zinc atoms entering the crystal from the gas phase are in the same state as the zinc atoms which occupied interstices as a result of the thermal dissociation of ZnO.

Calcination in vacuum at temperatures below 700°C decreases the zinc concentration with respect to the initial ZnO. Decomposition is most intense at temperatures above 800°C. Subsequently, evaporation of zinc atoms starts to predominate:

$$2ZnO \rightarrow 2Zn\ (vapor) + O_2.$$

The luminescence, chemical, and electrical properties of zincite are interrelated and depend on the amount of superstoichiometric zinc.

The electroluminescence of ZnO depends on the composition of the surface layer and at the treatment temperature it changes simultaneously with the catalytic activity [11]. Two visible-range luminescence bands are characteristic for ZnO: green peaking at about 510 μm and yellow peaking at 620 μm (a red band is observed in some cases). The green band is ordinarily attributed to the presence of superstoichiometric zinc in the lattice. The yellow luminescence band is observed in ZnO samples calcined in atmospheric oxygen [9].

Analysis of the electron density distribution in the lattice of zincite crystals before and after calcination in zinc vapor showed that the excess zinc atoms occupy octahedral voids in the structure. ZnO crystals heated in zinc vapor contain $(15 – 16) \times 10^{19}$ zinc atoms/cm^3. The cell-parameter ratio c/a of zincite crystals changes from 1.6019 in the initial crystals to 1.6025 in crystals containing excess zinc [11].

In ZnO samples treated in zinc vapor at 1000°C the concentration of superstoichiometric zinc atoms is $\delta = 3.6 \times 10^{-4}$. At temperatures below 1000°C a high fraction of the zinc atoms located in octahedral voids are electrically neutral. Above 1400 – 1700°C almost all zinc occupying interstices is ionized.

Red ZnO forms when ammonium nitrate and zinc taken in the ratio 2 : 1 are calcinated (about 100°C). The experimental density of red ZnO crystals is identical to that of zincite 5.63 – 5.67 g/cm^3. The x-ray diffraction data of this ZnO correspond to, just as for zincite, a hexagonal unit cell with $a = 3.243(7)$ Å and $c/a = 1.605$ Å. Chemical analysis of red zinc samples showed that the color is due to the presence of superstoichiometric zinc in the lattice [12].

Prolonged calcination of zincite crystals in zinc vapor at temperatures above 800°C also leads to red coloration and higher conductivity. Additional calcination at 500 – 600°C does not change the color which appeared but it does cause a sharp drop of the conductivity. The coloration vanishes only after prolonged calcination at 900°C in air.

Zincite crystals can be synthesized by different methods: from the gas phase (needle crystals), crystallization of ZnO from a fluxed solution of PbF_2 (plate crystals). However, the properties of the crystals grown by these methods do not permit using the crystals in technology. The hydrothermal method has turned out to be more promising for obtaining high-quality isometric crystals.

Crystallization of zincite has been investigated in detail in chloride and alkali solutions. The best chloride solution has turned out to be NH_4Cl (4 – 10 wt.%). Intense recrystallization starts in them at 200°C. However, the size of the crystals grown did not exceed several millimeters [13].

Hydrothermal crystallization of zincite often occurs under reducing conditions because of the appearance of hydrogen due to the oxidation of the walls of the autoclave by water and especially alkali. In the case of alkali the hydrogen pressure reaches 6 – 8 MPa [14]. Hydrogen strongly affects the properties of the crystals, degrading their quality. Zincite crystals synthesized under such conditions possess low resistance. This is due to the destruction of the stoichiometric composition of ZnO. To obtain high resistance zincite crystals are grown in the presence of oxidizers ($KClO_3$, $KMnO_4$). The resistivity of the zincite crystals synthesized under such conditions increases by 2 – 3 orders of magnitude [14].

High resistivity ($10^{10}\ \Omega \cdot$ cm) of the zincite crystals hydrothermally grown in [15] from a solution containing KOH and LiOH was obtained after calcination in air or oxygen for 50 h at 800°C.

ZnO crystals grown in NH_4Cl solutions at 450°C and pressure 60 MPa have been studied in [16]. Spontaneous crystallization was accomplished on a wire lying on the axis of an autoclave and on the walls of the autoclave. For NH_4Cl content above 4% mainly long needle crystals grew. Prismatic thickened crystals predominated with about 3% NH_4Cl in the solution. Together with prismatic green zincite ZnO crystal, colorless plate-shaped crystals formed. The authors of the work proposed that the colorless crystals are a new modification of ZnO.

We indexed (Table 1) the lines of the powder pattern of the new modification of ZnO, except for the line with interplanar distance 2.150 Å, in the primitive monoclinic cell with $a = 6.896(14)$ Å, $b = 6.387(19)$ Å, $c = 5.468(21)$ Å, $\beta = 99.25(33)°$, $V = 237.7$ Å^3. For $Z = 10$ the computed density is 5.684 g/cm^3, which is in good agreement with the experimental data for zincite [12, 15]. This variant of indexing improves the previous result obtained in [17].

Perfect isovalent isomorphism of bivalent iron (0.78 Å) with zinc (0.74 Å) is observed in ionic compounds and minerals. The sphalerite lattice (Zn, Fe)S can contain up to 20 at.% Fe from the sum (Fe + Zn). The line with interplanar distance 2.150 Å is the most intense diffraction line of

TABLE 1.

I	d_e, Å	hkl	d_w, Å
1	3.390	200	3.392
3	3.110	– 201	3.111
2	2.890	120	2.891
10	2.660	– 102	2.665
5	2.460	– 112	2.460
2	2.300	202	2.305
3	2.150	–	–
1	2.030	130	2.032
5	1.910	122	1.909
5	1.680	321	1.680
9	1.570	023	1.569
6	1.480	141	1.480
6	1.350	403	1.350
1	1.170	214	1.170

wüstite $Fe_{1-x}O$ [ICPDS 84-0302]. This suggests that the green color is due to chromophoric bivalent iron ions entering the lattice.

$A^{II}B^{VI}$ compounds crystallizing under normal conditions in sphalerite or wurtzite structure undergo at high pressure a polymorphous transformation into a NaCl type structure. The restructuring of a wurtzite lattice structure into a sodium chloride lattice structure is accompanied by a change of the coordination number of the cation from four to six and a transition from hexagonal packing of the anions to close cubic packing. It can be realized by the anionic layers sliding relative to one another followed by displacement of the cations which initially occupied interstitial voids in the anionic lattice (see Fig. 1).

According to the data of [5] the difference of the crystal lattice energies of the phases with wurtzite and sphalerite structure is negligible. The phase with sphalerite structure possesses the same packing of anions as the phase with the sodium chloride structure. According to Ostwald's rule (1897) for stepped transitions a phase with sphalerite structure should form with decreasing pressure, which conforms to the experimental data. A structural transformation from wurtzite into NaCl structure in cadmium chalcogenides (CdS, CdSE, CdTe) is observed at low pressures.

The polymorphous transformation CdS ($P6_3mc$) → CdS (Fm3m) under dynamic [18] and static [19, 20] compression proceeds rapidly and, evidently, is diffusion-free. In CdS the phase transition ($P6_3mc$ → Fm3m) occurs at room temperature and pressure about 2 GPa.

After pressure is lowered, the yellow color characteristic for cadmium sulfide with wurtzite structure changed to red, which is characteristic of CdS with sphalerite structure. The diffraction peak in the x-ray diffraction patterns of CdS obtained after reaching pressure 0.1 MPa largely corresponded to the phase with sphalerite structure. The CdS phase with a hexagonal wurtzite structure was present in small quantities. Thus, in accordance with Ostwald's rule of stepped transitions with decreasing pressure a sequence of polymorphous transformations accompanied by a change of structure is observed in CdS: NaCl type (Fm3m) → α-ZnS type ($F\bar{4}3m$) → β-ZnS type ($P6_3mc$). If NaCl is introduced into the initial CdS ($P6_3mc$) (2 : 1 mass ratio), then the high-pressure phase of CdS (about 50 wt.%) remains under normal conditions.

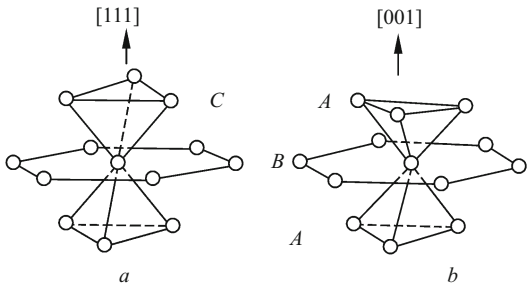

Fig. 1. Orientation of the coordination tetrahedra in sphalerite (*a*) and wurtzite (*b*).

The high-pressure phase (Fm3m) CdSE is more difficult to preserve in the metastable state and it is impossible to preserve CdSe [19, 20].

We expect that the above-described phase transformation of cadmium sulfide at high pressure in the presence of NaCl can serve as an illustration of the universal symmetry principle stated by P. Curie, who studied symmetry as a state of the space that is characteristic for the medium where a given phenomenon occurs. He noted that the characteristic symmetry for any particular phenomenon is the maximum symmetry of the medium that is compatible with the existence of the phenomenon. A phenomenon can exist in a medium which possesses either characteristic symmetry or one of its subgroups [21]. The symmetry of the surrounding medium is seemingly imprinted on the object formed in it.

At room temperature and high pressure sphalerite undergoes a polymorphous transformation ZnS($F\bar{4}3m$) → ZnS(Fm3m). This phase transition is determined at pressure 16.4 GPa and is used for calibrating high-pressure chambers. The reverse transformation is observed at pressure 10 – 11 GPa [22]. The unit cell parameter of ZnS(Fm3m) at 18 GPa equals 4.990 Å. The transformation occurs with a volume jump $(\Delta V/V_0) = 21.2\%$ [23]. In the case of dynamic compression the structural change ZnS($F\bar{4}3m$) → ZnS(Fm3m) is observed at pressure 16 GPa [24].

At 10 GPa and 200°C zincite partially (about 30 wt%) transforms in the presence of NH_4Cl into a polymorphous modification of ZnO with NaCl type structure. In contrast to most other $A^{II}B^{VI}$ compounds the high-pressure phase of ZnO remained after the pressure was lifted. The lines of the x-ray diffraction patterns of the high-pressure phase were indexed in the cubic face-centered unit cell with $a = 4.280$ Å, $V = 78.4$ Å^3, $Z = 4$, $c = 6.892$ g/cm^3, volume per formula unit $(V/Z) = 19.6$ Å^3, and volume jump – 17.9% [25].

The quantity dP/dT was found to be positive along the line of transformation. According to the Clausius – Clapeyron equation, $dP/dT = \Delta S/\Delta V = \Delta H/T\Delta V$, which imposes definite thermodynamic conditions on the temperature dependence of the transition [26]. The enthalpy and entropy were calculated in [25]. The enthalpy was found to be 785 cal/mole at 25°C, while the entropy was only 2.6 cal/(mole · K).

The substance NH_4Cl crystallized under normal conditions in a CsCl type structure. At high pressure and temperature NH_4Cl transforms into a modification with NaCl structure [26].

The presence of a phase of NH_4Cl with a cubic face-centered lattice in accordance with P. Curie's symmetry principle, probably enabled the structural change of zincite and preserved the high-density phase of zincite ZnO after the pressure decreased.

In the present work we present the results of an x-ray diffraction study of the preserved phases of ZnO, which were formed after shock-wave compression of ZnO with the wurtzite structure.

Shock-wave compression is realized under impact and detonation of a condensed explosive in contact with the initial material. Under shock compression a pressure jump (about 10^{10} Pa) arises in the material and propagates through the materials at a high velocity (about 10^3 m/sec). The rise time of the pressure from the normal value (0.1 MPa) to the maximum value is $10^{-10} – 10^{-12}$ sec and the pressure drop-off (unloading) time is $10^{-5} – 10^{-6}$ sec. The pressure obtained in the experimental substance depends on the product of the shock-wave velocity D in it by its initial density ρ_0 and by the velocity u of the mass of the material: $P = \rho_0 Du$.

X-ray diffraction studies in the pulsed regime made it possible to detect the formation of the high pressure phase of BN at the moment the shock-wave passed. Under shock compression high-pressure phases were synthesized in microseconds — diamond, stishovite, and cubic boron nitride. The high-pressure phase of SiO_2 with stishovite structure was found in the products of decomposition of the substances Al_2SiO_5, Mg_2SiO_4, and $ZrSiO_4$ subjected to shock-wave compression. The high-pressure phase of BN was synthesized with shock-wave compression of the compound $BH_3 \cdot NH_3$. The x-ray diffraction identification of these phases attests to the formation of quite large crystallites (> 100 Å).

The part of the shock wave in which a jump occurs in the parameters of the medium (pressure, density, temperature, entropy) up to the maximum value is called the wave front. The region where this occurs is very small. According to Ya. B. Zel'dovich, for shock waves propagating in gas its extent is $10^{-5} – 10^{-8}$ cm. These values are small compared with the depth of the compression zone. The parameters of the medium behind the shock front can remain constant, for example, with supersonic motion of the body or decrease as in the case of the detonation of an explosive charge on the surface of metal barrier. In this case a region of rarefaction forms behind the shock wave and a rarefaction wave propagates right behind the shock wave. Tensile stresses (negative pressures) arise in rarefaction waves and give rise in the material to spallation phenomena (cleavage, fragmentation) and deformation as well as martensite phase transformations in which a coherent displacement of all atoms by a very small amount is possible. Graphite, graphite-like boron nitride, and zinc sulfide are substances which undergo a martensite transformation under shock compression.

Phase transformations with a decrease of density can occur in regions of negative pressure. These transformations can occur under static loading of a material. Phase transitions with a decrease of the density occur under static compression and shear as well as during comminution of the material in a ball mill [27].

Under the action of shock waves the formation of new phases, both diffusion-free and accompanied by mass transfer, are completed in fractions of a microsecond. Phase transformations at lower pressures and temperatures than under static conditions have been observed in a shock wave. This is promoted by intense plastic shear, which activates dislocation mechanisms, which, in turn, substantially increase the concentration of vacancies which accelerate diffusion.

The density of dislocations which arise as a result of deformation increases with increasing pressure of the shock wave. Under the action of a shock wave a high concentration of defects arises in the material, as a result of which long-range order is not preserved, and after unloading the material transforms into an amorphous state.

When a shock wave transforms a material into a compressed state, strong plastic deformation occurs. The subsequent unloading wave produces the same plastic deformation as does the loading wave. Time-varying regions of local stresses and deformations are formed; these regions promote the initiation of a destruction process in one part of the body irrespective of what happens in another part.

Under compression by a shock wave the temperature of a material increases according to the pressure in the wave front. Intensification of shock compression is accompanied by a temperature increase such that after unloading the residual temperatures can reach hundreds and even thousands of degrees. When a material loaded by a shock wave cools from the residual temperature the same phase and structural transformations can occur as during ordinary heat treatment but with a higher cooling rate. The fragmented particles begin to re-sinter, and their internal defect density decreases. In the process the crystal lattice becomes more perfect. The most stable phase under these conditions crystallizes from the melt. The energy transferred by the shock wave to the material raises the temperature the most and does not decrease the volume.

If the pressure gradient is sufficiently large, the shock front can be compared to a mill. Large pressure gradients in a shock front result in substantial comminution of the particles of very strong substances. After comminution by shock

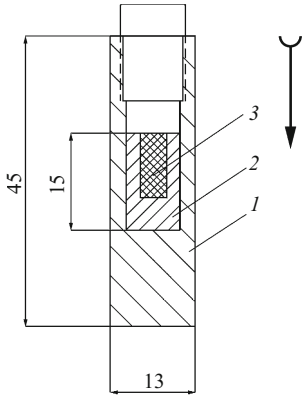

Fig. 2. Storage ampul.

waves the regions of coherent scattering decrease substantially and are characterized by high microstresses.

The existence of crystalline order in the matter behind a shock front was established in [28]. Diffraction peaks from the (111) and (200) planes of aluminum compressed by a shock wave (14 GPa) were recorded.

A substantial time elapses from the moment a material in a metal hermetic container (storage ampul) is compressed until its physical – chemical characteristics are studied. The processes occurring in the storage ampul are much more complex than the phenomena occurring during the passage of the shock wave. In most cases the post-compression structure of the material does not correspond to the structure that was present behind the shock front.

Facilities for shock-wave loading are divided according to geometry into planar, axisymmetric (cylindrical), and spherical (with central symmetry). In the latter two geometries the phenomenon of cumulation is used because converging shock waves are created in the sample.

In our work shock-wave action on zincite occurred under axisymmetric loading in a steel storage ampul [29]. The construction of the explosive charge and storage ampul are described in [30].

Zincite (GOST 1062–73) with mass 0.38 g was placed (Fig. 2) into a narrow channel *1* (diameter 4 mm) of a thick-walled copper vessel *2* (8 mm in diameter), arranged coaxially along the axis of a steel cylindrical ampul *3* (outer diameter 13 mm). To prevent spallation phenomena from destroying the storage ampul its bottom end was place in contact with a thick steel plate.

Shock-wave compression was achieved by a sliding detonation wave from the detonation of a cylindrical charge consisting of an alloy of trotyl and desensitized hexogen (40/60 wt.%) with density 1.68 g/cm^3 placed inside a steel shell. A plane-wave generator consisting of 0.1 g lead azide initiated the detonation.

The preserved products of shock-wave compression were studied in an FR-552 focusing monochromator chamber with Cu$K_{\alpha 1}$ radiation (germanium was the internal standard).

TABLE 2.

I	d_e, Å	*hkl*
15	3.5700	100
7	2.9155	103
1	2.5916	104
1	2.5227	006
100w*	2.0581	110
		106
1	1.9890	112
2	1.7850	200
15	1.4561	206
1	1.3923	118
		1010
1	1.2975	208
2	1.2598	0012
1	1.1873	1012

* Wide.

The diffraction lines of new phases were found in the diffraction patterns of two preserved samples of ZnO(I, II) together with the lines of zincite: ZnO(I), ZnO(II), and ZnO(III). The intensities of the diffraction lines were evaluated according to the blackening marks and placed on a 100-point scale.

The x-ray data on the ZnO(I) phase were indexed in the hexagonal unit cell (Table 2) with $a = 4.121(2)$ Å, $c = 6c_0\,(2.519) = 15.114(5)$ Å, $V = 222.3$ Å^3. The hexagonal lattice of ZnO(I) can be regarded as a distorted cubic face-centered lattice of ZnO($F\bar{4}3m$) [8]. The vectors of the hexagonal cell $\vec{a}_h$, $\vec{b}_h$, $\vec{c}_h$ are related with the vectors of the cubic cell $\vec{a}_c$, $\vec{b}_c$, $\vec{c}_c$ by the following relations:

$$\vec{a}_h = 1/2\vec{a}_c - 1/2\vec{b}_c$$

$$\vec{b}_h = 1/2\vec{b}_c - 1/2\vec{c}_c$$

$$\vec{c}_h = 3/2\vec{a}_c + 3/2\vec{b}_c + 3/2\vec{c}_c.$$

The matrix for the transformation of the cubic-cell vectors and the calculation of the indices *hkl* of the planes in the hexagonal cell (see Table 2) has the form

$$\begin{vmatrix} 1/2 & -1/2 & 0 \\ 0 & 1/2 & -1/2 \\ 3/2 & 3/2 & 3/2 \end{vmatrix}.$$

The parameters of the hexagonal cell of ZnO(I) calculated according to this matrix for $\vec{a}_c = 5.816$ Å are $a = 4.113$ Å and $c = 15.111$ Å.

The systematic extinctions of the reflections in the x-ray pattern of ZnO(I) correspond to the Fedorov groups $P6_3/mmc$, $P6_3mc$, and $P\bar{6}2c$. The first two belong to eight

Fedorov groups describing the symmetry of the structures constructed according to tight packing of spheres. The symmetry of *n*-layer tight packings is a multiple of the order of the Fedorov group. The two-layer, four-layer, and one of the six-layer tight packings possess $P6_3/mmc$ symmetry. In the group $P6_3/mmc$ the symmetry value of four positions is 2, two positions 4 and 6, and three position 12. The points of the general position occupy the position with symmetry value 24 (order of the group). In the group $P6_3mc$ the symmetry values of three positions are 2, 4, and 6, respectively. Three positions have the same symmetry value 12. For the group $P\bar{6}2c$, just as for $P6_3/mmc$, four positions have symmetry value 2 and two positions have values 4 and 6. The order of the group is 12 (the points of the general position).

For $Z = 12$ (symmetry value) the molecular volume of ZnO(I) (V/Z) equals 18.52 Å^3, and the computed density is 7.293 g/cm^3. This is 5.82% larger than the density of the phase ZnO ($Fm\bar{3}m$), synthesized under static compression in [25]. The volume jump at the phase transition ZnO ($P6_3mc$) $\rightarrow$ ZnO(I) equals – 22.8%.

A transition from the hexagonal cell of ZnO(I) to the monoclinic cell with 3 times smaller volume is possible: $a = 4.118$ Å, $b = 4.112$ Å, $c = 4.362$ Å, $\beta = 101.1°$, $V = 72.8$ Å^3, with $Z = 4(V/Z) = 18.2$ Å^3.

The matrix of the transformation from hexagonal to monoclinic cells is

$$\begin{vmatrix} 1/4 & 1/2 & -1/4 \\ -1 & 0 & 0 \\ 1/2 & 1 & 1/6 \end{vmatrix}.$$

The monoclinic cell can be regarded as a cubic face-centered cell of ZnO compressed along the *a* and *b* axes and elongated along the *c* axis [25].

The phase ZnO(I) is probably one of the high-density polytypes of ZnO ($P6_3/mmc$), which are formed under nonhydrostatic stresses, compression and shear.

Analysis of the x-ray diffraction data for sample II (Table 3) shows that this is a mixture of two structurally close phases ZnO(II) and ZnO(III). The x-ray diffraction data for the ZnO(II) phase were indexed by the homology method. A hexagonal lattice corresponding tight packing was taken as the base of the initial lattice. A distortion of the lattice can be accompanied (because of the displacement of the atoms) by the appearance of weak additional lines which are absent in the x-ray diffraction pattern of the material with the initial structure.

The arrangement of the series of intense lines corresponds to a C-basocentered orthorhombic subcell. For this distortion the line 100 of the hexagonal cell splits into two lines — 110 and 200, the line 101 into 111 and 200, and the line 101 into 111 and 201. The lines 001 and 002 of the hexagonal cell do not split. The index 110 corresponds to the first diffraction line in the diffraction pattern of ZnO(II), 200 to the second, 001 to the third, 111 to the fourth, 220 to the fifth, and 310 to the sixth. However, the lines with interplanar distances 1.7556 and 1.4421 Å are indexed with indices that do not correspond to a C-basocentered orthorhombic subcell (see Table 3).

TABLE 3.

I	d_e, Å	*hkl*	
		monoclinic cell	orthorhombic subcell
13	3.9630	200	110
		020	–
30	2.9970	001	200
8	2.3885	021	–
10	2.3690	201	001
100	2.2718	211	–
10	2.0317	221	111
3	1.9776	040	220
25	1.8677	330	310
23	1.7556	–	030
22	1.6396	401	–
6	1.5554	510	–
28	1.4421	112	410
7	1.3278	– 222	–
3	1.3130	222	–
5	1.2300	531	–
5	1.2057	– 402	240

The parameters of the orthorhombic subcell were determined from the indexed lines: $a = 5.997(2)$ Å, $b = 5.267(1)$ Å, $c = 2.369(1)$ Å, $V = 74.8$ Å^3, $Z = 4$, $\rho_{calc} = 7.222$ g/cm^3.

The x-ray diffraction data for ZnO(III) were indexed in the primitive monoclinic unit cell with $a = 7.932(8)$ Å, $b = 7.911(4)$ Å, $c = 2.995(1)$ Å, $\beta = 91.07(4)°$, $V = 187.9$ Å^3, $Z = 8$, $(V/Z) = 23.47$ Å^3, $\rho_{calc} = 5.751$ g/cm^3. This monoclinic cell is associated with a distorted (triclinic) cubic face-centered cell of ZnO ($F\bar{4}3m$) with equal volume.

The matrix of the transformation to the triclinic cell has the form

$$\begin{vmatrix} -1/2 & 1/2 & 0 \\ 1/2 & 1/2 & 0 \\ 0 & 0 & -2 \end{vmatrix}.$$

The parameters of the triclinic cell are $a = 5.603$ Å, $b = 5.603(4)$ Å, $c = 5.992$ Å, $\alpha = 89.4°$, $\beta = 90.74°$, $\gamma = 90.15°$, $V = 188.1$ Å^3.

In summary, three new polymorphous modifications of zinc oxide were synthesized by dynamic compression of zincite (28 GPa). Two of these modifications are high-density. Just as in cadmium chalcogenides, the high-density phases of ZnO form with the participation of a phase with sphalerite structure — ZnO ($F\bar{4}3m$).

The work is dedicated to the memory of B. S. Svetlov, professor at the D. I. Mendeleev Russian Chemical Technology University and a prominent Russian scientist who made a large contribution to study of the kinetics of chemical reactions.

REFERENCES

1. L. A. Reznitskii, *Crystal Energetics of Oxides* [in Russian], Izd. MGU, Moscow (1998).
2. N. V. Belov, Yu. G. Zagal'skaya, G. P. Litvinskaya, and Yu. K. Egorov-Tismenko, *Atlas of Space Groups of the Cubic System* [in Russian], Nauka, Moscow (1980).
3. A. N. Tsvigunov, A. S. Krasikov, and V. G. Khotin, "Simultaneous shock-wave synthesis of precious spinel and a cubic Laves phase," *Steklo Keram.*, No. 6, 21 – 22 (2006); A. N. Tsvigunov, A. S. Krasikov, and V. G. Khotin, "Combined shock-wave synthesis of noble spinel and Laves cubic phase," *Glass Ceram.*, **63**(5 – 6), 196 – 197 (2006).
4. V. L. Tauson and L. V. Chernyshov, *Elementary Investigations in Crystal Chemistry and Geochemistry of Zinc Sulfide* [in Russian], Nauka, Novosibirsk (1981).
5. E. Lombardi and L. Jensen, "Stability of crystals of II-VI and III-V compounds in terms of three-ion interactions," *Phys. Rev. A*, **10**(1), 275 – 292 (1965).
6. G. A. Jeffrey, G. S. Parry, and R. L. Mozzi, "Study of wurtzite-type binary compounds. I. Structures of aluminum nitride and beryllium oxide," *J. Chem. Phys.*, **25**(5), 1024 – 1031 (1956).
7. S. C. Abrahams and J. L. Bernstein, "Remeasurement of the structure of hexagonal ZnO," *Acta Cryst.*, **25**(7), 1233 – 1236 (1969).
8. O. E. Radczewski and R. F. Schicht, "Bestimmung der Gitterkonstante von Kubischem Zinkmonoxyd," *Nartursissenschaften*, **56**(10), 514 (1969).
9. M. N. Lanchevskaya, G. P. Panasyuk, and N. I. Kobozev, "Effect of superstoichiometric zinc on the properties of zinc oxide. Luminescence," *Zh. Fiz. Khim.*, **62**(11), 2843 – 2846 (1968).
10. I. K. Vereshchagin, "On the relation between the luminescence electric and chemical properties of zinc oxide," *Izv. Vyssh. Uchebn. Zaved. Ser. Fiz.*, No. 2, 31 – 36 (1960).
11. G. P. Mohanty and L. V. Azaroff, "Electron density distributions in ZnO crystal," *J. Chem. Phys.*, **35**(4), 1268 – 1270 (1961).
12. W. Ehret and A. Greenstone, "Red zinc oxide," *J. Amer. Ceram. Soc.*, **65**(5), 872 – 877 (1949).
13. V. A. Kuznetsov and A. N. Lobachev, "Hydrothermal method of growing crystals," *Kristallografiya*, **17**(4), 878 – 904 (1972).
14. I. P. Kuz'mina, A. N. Lobachev, and N. S. Triodina, "Study of the hydrothermal synthesis of zincite," in: *Investigation of Crystallization Processes under Hydrothermal Conditions* [in Russian], Nauka, Moscow (1970), pp. 29 – 42.
15. E. D. Kolb and R. R. Laudisse, "Properties of lithium-doped hydrothermally grown single crystals of zinc oxide," *Amer. Ceram. Soc.*, **48**(7), 342 – 345 (1965).
16. D. Rikl and J. Bauer, "Hydrotermalsynthese von Zinkit," *Kristall und Techn.*, **3**(9), 375 – 384 (1968).
17. A. N. Tsvigunov, "New modification of hydrothermally synthesized zinc oxide," *Steklo Keram.*, No. 8, 17 – 19 (2001); A. N. Tsvigunov, "A new modification of zinc oxide synthesized by the hydrothermal method," *Glass Ceram.*, **58**(7 – 8), 280 – 282 (2001).
18. J. D. Kennedy and W. B. Benedick, "Shock-induced phase transition in single crystal CdS," *Phys. Chem. Solids*, **27**(11), 125 – 127 (1966).
19. K. Rumans, *Structural Studies of Some oxides and Other Chalcogenides under Normal and High Pressures* [Russian transtaltion], Mir, Moscow (1969).
20. L. F. Vershchagin and S. S. Kabalkin, *X-ray Diffraction Studies at High Pressure* [in Russian], Nauka, Moscow (1979).
21. P. Curie, *Collected Works* [Russian translation], Nauka, Moscow (1966).
22. T. Yagi and S. Akimoto, "Pressure fixed points between 100 and 200 kbar based on the compression of sodium chloride," *J. Appl. Phys*., **47**(7), 3350 – 3354 (1976).
23. P. L. Smith and J. E. Martin, "The high-pressure structures of zinc sulfide and zinc selenide," *Phys. Lett.*, **19**(7), 541 – 543 (1965).
24. W. H. Gust, "Shock induced transition stresses for zinc sulfide and zinc selenide," *J. Appl. Phys*., **53**(7), 4843 – 4846 (1982).
25. C. H. Bates, W. B. White, and R. Roy, "New high-pressure polymorph of zinc oxide," *Science*, **137**(3534), 993 (1962).
26. A. J. Majudar and R. Roy, "Test of the applicability of the Clapeyron relationship to a few cases of solid – solid transitions," *Inorg. Nucl. Chem.*, **27**(9), 1961 – 1973 (1965).
27. A. N. Tsvigunov, L. M. Kovda, E. V. Zubova, et al., "On the influence of non-hydrostatic stresses on phase transformations of uranous-uranic oxide at room temperature," *Dokl. Akad. Nauk SSSR*, **210**(2), 365 – 366 (1972).
28. L. A. Egorov, É. V. Nitochka, and Yu. K. Orekin, "Recording powder patterns of shock-compressed aluminum," *Pis'ma Zh. Éksp. Teor. Fiz.*, **16**(1), 8 – 10 (1972).
29. G. A. Adadurov, A. N. Dremin, G. I. Kannel', et al., "Determination of the parameters of shack waves in matter preserved in cylindrical ampuls," *Fiz. Gor. Vzryva*, **3**(2), 281 – 285 (1967).
30. A. N. Tsvigunov, V. G. Khotin, A. S. Krasikov, et al., "Synthesis of a new modification of aluminum oxide with spinel structure by shock-wave loading of gibbsite," *Steklo Keram.*, No. 8, 16 – 18 (1999).